

Study of electron transfer interaction between hypocrellin and *N,N*-diethylaniline by UV–visible, fluorescence, electron spin resonance spectra and time-resolved transient absorption spectra

Man-Hua Zhang^{a,*}, Min Weng^a, Shen Chen^a, Wan-lin Xia^a, Li-Jing Jiang^a, De-Wen Chen^b

^a Institute of Photographic Chemistry, Academia Sinica, Beijing 100101, China

^b National Laboratory for Structural Chemistry of Unstable and Stable Species, Beijing 100083, China

Received 25 July 1995; accepted 1 November 1995

Abstract

Hypocrellin A (HA) and hypocrellin B (HB) extracted from *Hypocrella bambusae* (B. et. Br) Sacc are perylene quinoid pigments. Quenching of HA or HB fluorescence by *N,N*-diethylaniline (DEA) results in Stern–Volmer plots; the quenching rate constants in CH₃CN are $2.28 \times 10^{10} \text{ M}^{-1} \text{ s}^{-1}$ for HA and $2.34 \times 10^{10} \text{ M}^{-1} \text{ s}^{-1}$ for HB and are in agreement with those calculated from the semiclassical Marcus theory. The values of the free energy change ΔG for electron transfer between HA* or HB* and DEA calculated from Weller's equation are -1.21 eV for HA and -1.24 eV for HB. Electron spin resonance (ESR) signals of semiquinone radical anions of HA or HB have been detected on illumination ($\lambda = 550 \text{ nm}$) of HA or HB and DEA in anaerobic dimethylsulphoxide and CH₃CN solutions, indicating that an electron transfer has occurred from the ground state of DEA to excited states of HA or HB. The UV–visible spectra of HA in the presence of DEA in dimethylformamide and the time-resolved transient absorption spectra of the interaction of HA and DEA in different concentrations of HA and DEA in CH₃CN are examined. The observation of transient absorption of the semiquinone radical anion of HA ($\lambda_{\text{max}} = 620 \text{ nm}$) is also evidence of this electron transfer process. The interaction of HA and *N*-ethylaniline, aniline is also studied by UV–visible, ESR and fluorescence spectra.

Keywords: Semiquinone radical anion of hypocrellins (HA^{•-} and HB^{•-}); DEA; ESR; Time-resolved transient absorption

1. Introduction

Hypocrellin A (HA) and hypocrellin B (HB) (Fig. 1) are obtained from *Hypocrella bambusae* (B. et. Br) Sacc, a Chinese herb which grows most abundantly in the southwestern part of China [1–3]. They possess potent photodynamic action and several other significant biological activities and have been utilized as efficient photochemotherapeutic agents for some skin diseases clinically [4]. Recently it has been found that HA has a strong photodynamic therapy of tumours [5,6]. Generation of reactive oxygen species such as singlet oxygen, superoxide anion and hydroxy radical by illumination of HA or HB in solutions has also been reported [7,8]. Some fundamental photophysical parameters of HA and HB have also been reported [9]. Other chemical and photophysical properties of hypocrellins have been summarized by Diwu [10].

Electron transfer between HA and amines has been studied through fluorescence quenching and photovoltage measure-

ment in our laboratory [11]. In this paper, examination of fluorescence, electron spin resonance (ESR) and UV–visible spectra and transient absorption spectra in solvents of various polarities provides further evidence for the electron transfer interaction between HA or HB and *N,N*-diethylaniline (DEA).

2. Experimental details

2.1. Materials

HA was supplied by Dali Pharmaceutical Factory, Yunnan Province, China, and was recrystallized twice from acetone. HB was transformed from HA [12]. DEA, *N*-ethylaniline (EA) and aniline (AN) were distilled under reduced pressure before use. All the other solvents used here were of analytical grade (supplied by Beijing Chemical Factory). The fluorescence emissions from the solvents used were measured before the experiments and were negligible.

* Corresponding author.

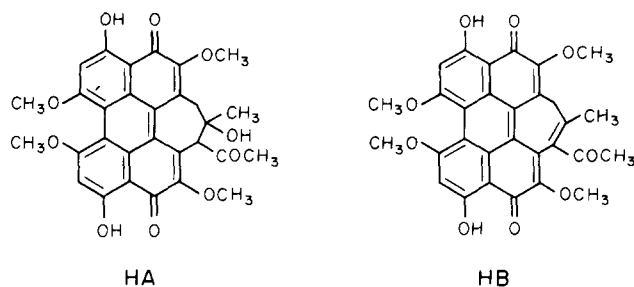
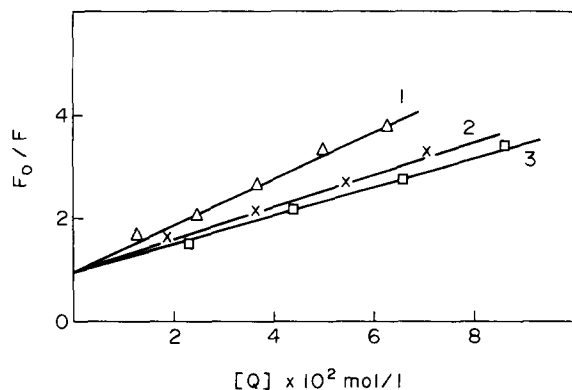


Fig. 1. The structures of hypocrellins HA and HB.

Fig. 2. Fluorescence quenching of HA by aromatic amines in CH_3CN ($[\text{HA}] = 4.8 \times 10^{-5} \text{ M}$; $\lambda_{\text{ex}} = 468 \text{ nm}$; $\tau = 1.57 \text{ ns}$ (in CH_3CN): curve 1, DEA, curve 2, EA, curve 3, AN).

2.2. Spectrometric measurements

ESR spectra were recorded using a Bruker ESP 300 spectrometer at room temperature. The samples were deoxygenated by flowing highly purified argon for 30 min and then were introduced into quartz capillaries and illuminated directly inside the microwave cavity with an unfiltered 450 W high pressure sodium lamp (maximum emission is around 550 nm). All the photoinduced ESR spectra were detected immediately after illumination. Ground state absorption measurements were made with a UV-160A UV-visible spectrophotometer; the samples were bubbled with highly purified argon for 30 min and irradiated with a 450 W high pressure sodium lamp and were then immediately examined. Steady state fluorescence quenching data were obtained for argon-

purged solutions of $1.2 \times 10^{-5} \text{ M}$ HA (HB) and aromatic amines (usually $(1-8) \times 10^{-2} \text{ M}$) with a Hitachi MPF-4 fluorescence spectrometer. Time-resolved fluorescence measurements were performed with a time domain fluorescence spectrometer HORIBA NAES-1100 model. The reduction potential values $E(\text{A}^-/\text{A})$ of the HA and HB (in volts against Ag/Ag^+) are the half-wave cathodic potentials, measured by cyclic voltammetry in polar solvents. The oxidation potential values $E(\text{D}^+/\text{D})$ for the aromatic amines are the half-wave anodic potentials taken from Ref. [13]. Time-resolved transient absorption spectra were measured with a Q-switched Nd:YAG nanosecond laser apparatus (full width at half-maximum, less than 5 ns; 35 mJ pulse^{-1} ; $\lambda = 355 \text{ nm}$). A xenon flash was used as an analysis flash for the detection of transients. The monitoring light passing through a grating monochromator was analysed by a detection system consisting of a photomultiplier tube and an oscilloscope. The samples in $2 \text{ mm} \times 10 \text{ mm}$ glass cells were bubbled with highly purified argon for 30 min before measurement.

3. Results and discussion

3.1. Fluorescence quenching and ΔG calculation

The fluorescence of HA and HB in dimethylsulphoxide (DMSO) and acetonitrile were effectively quenched by DEA. In acetonitrile there was no change in the shape of the fluorescence spectra, even with the highest concentration of the quenchers used. Thus it was expected that, in this solvent, no exciplex was involved in the quenching mechanism. Within the low concentration limit of the quenchers, the steady state fluorescence quenching followed the Stern-Volmer (SV) relationship [14] (the quenching curves are shown in Fig. 2):

$$I_0/I = 1 + K_{\text{sv}}[Q] = 1 + k_{\text{q}}\tau_0[Q] \quad (1)$$

where I_0 and I are the relative fluorescence intensities in the absence and presence of the quencher (Q), τ_0 is the fluorescence lifetime of the fluorophore in the absence of the quencher and k_{q} is the bimolecular quenching constant. The

Table 1
Bimolecular quenching constants obtained by steady state time-resolved fluorescence measurements and theoretical calculation

Quencher	Solvent	Steady state k_{q} ($\times 10^{10} \text{ M}^{-1} \text{ s}^{-1}$)		Time-resolved k_{q} ($\times 10^{10} \text{ M}^{-1} \text{ s}^{-1}$)		Theoretical value of k_{q} ($\times 10^{10} \text{ M}^{-1} \text{ s}^{-1}$)		Change ΔG in free energy (eV)	
		HA	HB	HA	HB	HA	HB	HA	HB
DEA	CH_3CN	2.28	2.34	2.10	2.21	1.92	1.94	-1.21	-1.24
	DMSO	1.39	1.53	1.33	1.56				
EA	CH_3CN	1.93	1.95	1.93	1.96	1.87	1.89	-1.15	-1.18
	DMSO	0.98	1.04	0.94	1.02				
AN	CH_3CN	1.89	1.93	1.90	1.95	1.84	1.87	-1.01	-1.04
	DMSO	0.56	0.58	0.53	0.56				

k_q values obtained from the slope of I_0/I vs. $[Q]$ plots are listed in Table 1.

The effect of the quenchers on the fluorescence lifetime τ of the HA and HB was also studied and a linear SV quenching was observed:

$$\tau_i/\tau = 1 + k_q\tau_0 \quad (2)$$

where τ is the fluorescence lifetime of the HA and HB in the presence of the quencher. The k_q values thus obtained for different fluorophore–quencher pairs are listed in Table 1 and are in agreement with those obtained from the steady state measurements, indicating that static quenching was not observed in the present system.

The standard free energies ΔG_{et} of electron transfer between the first excited state of HA or HB and aromatic amines were calculated from Weller's equation [15,16]:

$$\Delta G = E(D^+/D) - E(A^-/A) - e_0^2/\epsilon_a - \Delta E_{0-0} \quad (3)$$

(e_0^2/ϵ_a in acetonitrile is 0.06 eV [16])

Photophysical and electrochemical properties of the HA or HB and aromatic amines are listed in Table 2.

The values of electron transfer rate constants calculated from the semiclassical Marcus theory [15–20] and from experiment are given in Table 1. Values of $k_q > 10^{10} \text{ M}^{-1} \text{ s}^{-1}$ were observed in all cases. They approached the rate of diffusion in acetonitrile solution and were in agreement with calculated values. We assumed that the fluorescence quenching of HA and HB in acetonitrile by DEA was due to electron transfer from the ground state DEA to the excited state HA and HB.

3.2. Electron spin resonance

Illumination of HB and DEA in Ar-gassed DMSO solution generated an ESR signal (Fig. 3, spectrum B). No signal was observed if DEA was omitted (Fig. 3, spectrum A). The ESR signal intensity of the $\text{HB}^{\cdot-}$ depends on the DEA concentration, oxygen, irradiation time and intensity. Oxygen quenched the ESR signal via single electron transfer to pro-

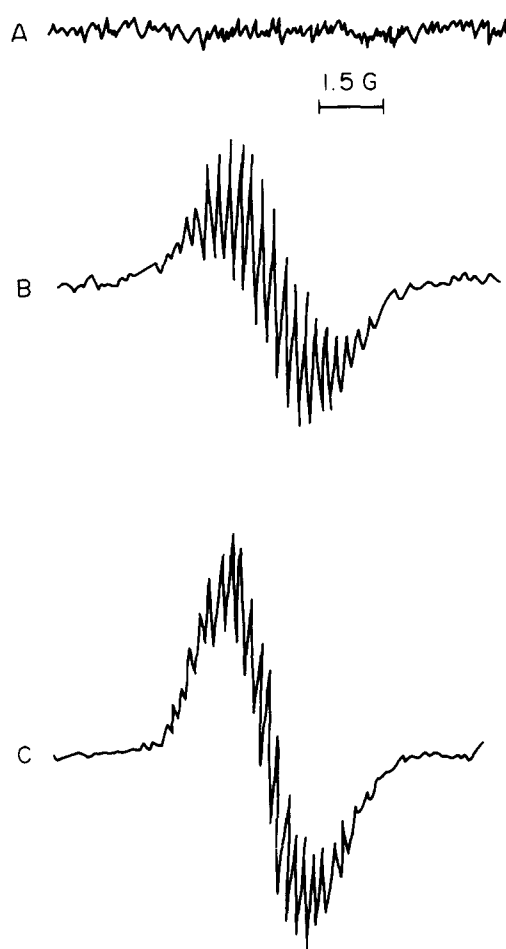


Fig. 3. Measured (spectra A and B) and simulated (spectrum C) ESR spectra. ESR spectra of the deaerated solutions containing HB ($2 \times 10^{-3} \text{ mol l}^{-1}$) in DMSO at room temperature (spectrometer settings: microwave power, 1.02 mW; modulation amplitude, 0.1 G; receiver gain, 5×10^5): spectrum A, DEA absent; spectrum B, DEA ($6 \times 10^{-2} \text{ mol l}^{-1}$) present. Spectrum C, computer-simulated ESR spectrum with $a_{\text{OH}}^{\text{H}} = 1.66 \text{ G}$ (1H), $a_{\text{aro}}^{\text{H}} = 0.46 \text{ G}$ (2H), $a_{\text{OCH}_3}^{\text{H}} = 0.225 \text{ G}$ (6H), $a_{\text{CH}_3}^{\text{H}} = 0.81 \text{ G}$ (3H), $a_{\text{CH}_2}^{\text{H}} = 0.85 \text{ G}$ (2H).

duce the superoxide anion radical ($\text{O}_2^{\cdot-}$). The signal with finely resolved structure and long lifetime (above 5 min) was attributed to the semiquinone radical anion from HB. The

Table 2
Photophysical and electrochemical properties of the hypocrellin A or hypocrellin B and aromatic amines

	$^1E_s^a$ (kJ mol^{-1} (eV))	$E(A/A^-)^b$ vs. Ag/Ag^+ (V)	τ_0^c (ns)	$E(D/D^+)^d$ vs. Ag/Ag^+ (V)
Fluorophores				
HA	199.6 (2.071)	-0.58	1.50	
HB	198.0 (2.054)	-0.53	1.02	
Quenchers				
DEA				0.34
EA				0.40
AN				0.54

^a Singlet energies of HA and HB, determined from the overlap of the normalized absorption and emission spectra.

^b Reduction potential of HA and HB in acetonitrile solution.

^c Fluorescence lifetimes of HA and HB in deoxygenated acetonitrile solution.

^d Oxidation potential of aromatic amines from Ref. [13].

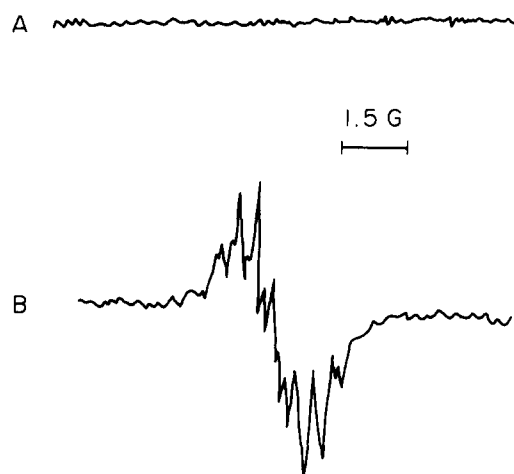


Fig. 4. ESR spectra of the deaerated solutions of HA ($2 \times 10^{-3} \text{ mol l}^{-1}$) at room temperature (spectrometer settings: microwave power, 1.02 mW; modulation amplitude, 0.1 G; receiver gain, 5×10^5): spectrum A, DEA absent in DMSO; spectrum B, DEA ($6 \times 10^{-2} \text{ mol l}^{-1}$) present in DMSO.

simulated spectrum is shown in Fig. 3, spectrum C, and was fitted to the experimental ESR spectra of $\text{HB}^{\cdot-}$. A similar result was obtained in CH_3CN . In our experiments a high pressure sodium lamp was used as a light source. Its maximum emission is around 550 nm. Because of no absorption of DEA around 550 nm, only HB could be excited there. So the most likely mechanism of generation of the semiquinone radical anion of HB was supposed to be acceptance of an electron by an excited state of HB from the ground state of DEA. Because of the similarities of structures and properties of HA and HB, electron transfer should also be possible from DEA to HA. The expected ESR signal of the semiquinone radical anion of HA generated from the photolysis of HA solution in the presence of DEA was also recorded (Fig. 4).

3.3. Absorption spectra

Absorption spectra of HA and HB have been reported in our laboratory. Three bands of HA with absorption maxima at around 468, 540 and 580 nm in the visible light area are observed; HB absorbed at 468, 542 and 580 nm. Addition of DEA did not affect the absorption spectra of HA, indicating the absence of ground state interaction between HA, HB and DEA. When HA in the deaerated solution of dimethylformamide (DMF) was irradiated in the presence of DEA, the absorbances of HA at 468, 540, and 580 nm continuously decreased while the 620 nm absorbance increased, making an isosbestic point at 583 nm (Fig. 5(a)). The presence of the isosbestic point at 583 nm showed that only two species, i.e. HA and its photoreduced product, existed. An et al. have reported that the absorption peak of $\text{HB}^{\cdot-}$ is at 618 nm [21]. We suggested that the photoreduced product of HA should be $\text{HA}^{\cdot-}$, and the absorption at 620 nm attributed to $\text{HA}^{\cdot-}$ is also mainly due to the following.

(i) The product was formed in the presence of a reductant, under irradiation and deaeration; when the air was caused to

re-enter the photoreduction system, the product was reversed back quantitatively to HA, and thus it is reasonable to believe that the product is photoreduced from HA.

(ii) The decay constant of the absorption at 620 nm and ESR signal of $\text{HA}^{\cdot-}$ were consistent in the dark (Fig. 5(b)); the same phenomena were obtained in DMSO.

3.4. Laser photolysis

The time-resolved transient absorption spectra of HA and DEA in different solutions are shown in Figs. 6 and 7. The three absorption bands, I ($\lambda = 510 \text{ nm}$), II ($\lambda = 560 \text{ nm}$) and III ($\lambda = 600 \text{ nm}$), were observed, while a change in solvent polarity caused slight shifts of the bands. Hu et al. have reported that triplet-triplet absorption of HB is composed of three bands ($\lambda_{\text{max}} = 510 \text{ nm}$, 560 nm, 600 nm respectively) in cyclohexane [22]; the lifetime of $^3\text{HA}^*$ is 4.3 μs . The time-resolved transient absorption spectra of HA and DEA in CHCl_3 (Fig. 6) showed that absorption maxima of bands I, II and III accorded with triplet-triplet absorption of HA very well; all three bands decayed by first-order kinetics with a lifetime of 6.0 μs and could be quenched by oxygen. Therefore it was reasonable to assign bands I, II and III to the triplet-triplet absorption of HA.

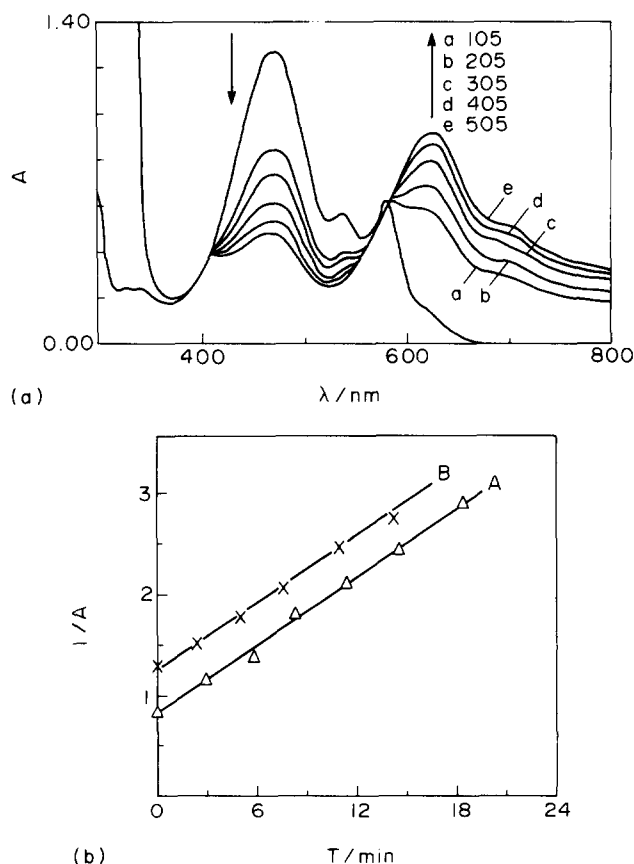


Fig. 5. (a) The absorption spectra changes observed on irradiation. Photoreduction of HA ($5 \times 10^{-5} \text{ mol l}^{-1}$) by DEA ($5 \times 10^{-3} \text{ mol l}^{-1}$) in deaerated DMF after 0 s, 10 s, 20 s, 30 s, 40 s, 50 s. (b) Intensity of ESR signal (curve A) and 620 nm absorption (curve B) from HA vs. darkness time in deaerated DMF ($[\text{HA}] = 5 \times 10^{-4} \text{ mol l}^{-1}$, $[\text{DEA}] = 5 \times 10^{-3} \text{ mol l}^{-1}$).

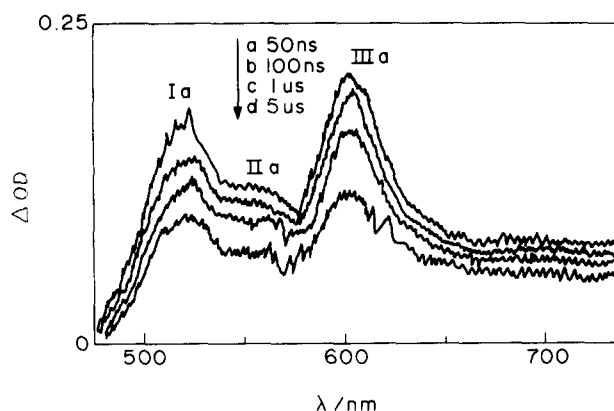


Fig. 6. Time-resolved transient differential absorption spectra of the interaction between HA and DEA in CHCl_3 at room temperature ($[\text{HA}] = 1.2 \times 10^{-4} \text{ mol l}^{-1}$, $[\text{DEA}] = 6.5 \times 10^{-3} \text{ mol l}^{-1}$, Ar saturated for 30 min, $\lambda_{\text{ex}} = 355 \text{ nm}$). The delay times after the pulses are shown above the spectra.

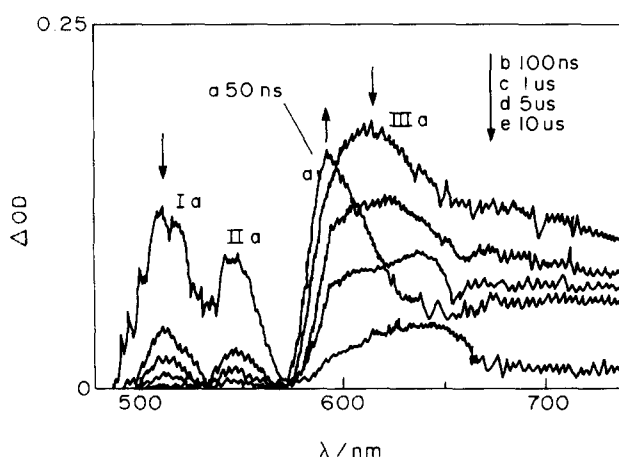


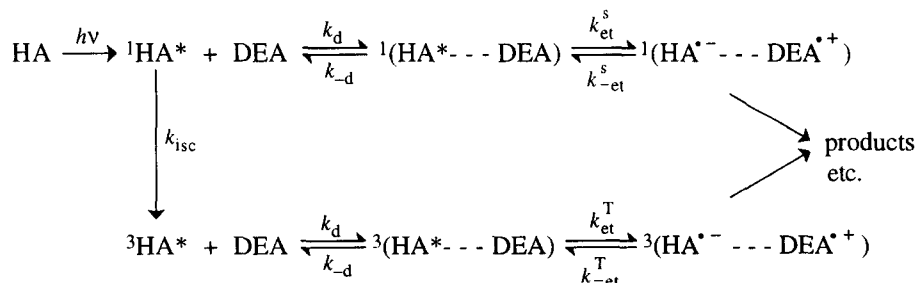
Fig. 7. Time-resolved transient differential absorption spectra of the interaction between HA and DEA in CH_3CN at room temperature ($[\text{HA}] = 3.5 \times 10^{-4} \text{ mol l}^{-1}$, $[\text{DEA}] = 6.7 \times 10^{-3} \text{ mol l}^{-1}$, Ar saturated for 30 min, $\lambda_{\text{ex}} = 355 \text{ nm}$). The delay times after the pulses are shown above the spectra.

Spectra quite different from those of Fig. 6 can be observed in Fig. 7, concomitant with the rapid decay of bands I and II ($\lambda_{\text{max}} = 510 \text{ nm}$, 560 nm respectively); band III ($\lambda_{\text{max}} = 600 \text{ nm}$) rose with some bathochromic effect from 200 ns to $1 \mu\text{s}$ following pulse excitation. This implied that band III in CH_3CN should not only be attributed to the triplet-triplet absorption of HA. In fact the analysis of the decay kinetics of band III indicated that band III consisted of two superim-

posed bands with different lifetimes ($\tau = 2.0 \mu\text{s}$ and $\tau = 8.9 \mu\text{s}$) and the shorter lifetime component was attributed to the triplet-triplet absorption of HA. An et al. have reported that the maximum absorption of the semiquinone radical anion of HA generated by steady state illumination of HA and systemine in DMF solution [21] is at 618 nm . Band III observed in Fig. 7 decayed with a bathochromic effect and the final maximum absorption was around 620 nm which agreed very well with the absorption of $\text{HA}^{\cdot-}$. Therefore the longer lifetime component of band III in CH_3CN could be reasonably assigned to absorption of the semiquinone radical anion of HA which underwent stabilization in a polar solvent (CH_3CN) and formation of a stable radical anion which could be detected by ESR and visible absorption spectra.

Unfortunately, the absorption of the radical cation of DEA was not observed. This might be because the unfavourable absorption position of the ground state HA prevented the identification of $\text{DEA}^{\cdot+}$ [23]. (The absorption spectrum of HA was shown in Fig. 5(a) and the absorption maximum is around 468 nm .)

Moreover, as mentioned above, the rate constant k_q of HA fluorescence quenching by DEA and the rate constant k_{isc} of intersystem crossing from S_1 to T_1 are $2.28 \times 10^{10} \text{ M}^{-1} \text{ s}^{-1}$ and $5.48 \times 10^8 \text{ s}^{-1}$ respectively. The electron transfer performs much more efficiently than intersystem crossing. However, at the concentration of DEA used in the system of Fig. 7, the fluorescence of HA was not quenched completely by DEA. The triplet-triplet absorption observed in Fig. 7 should result from incomplete quenching of singlet excited HA that underwent intersystem crossing to the triplet excited state. Nevertheless, the triplet-triplet absorption of HA in Fig. 7 decayed more rapidly with a relative short lifetime ($\tau = 2.0 \mu\text{s}$), indicating that the triplet state of HA might also be quenched by DEA. We have previously reported that the energy of the lowest triplet state of HA is very close to its lowest singlet excited energy [24]. The overall free energy change for electron transfer between DEA and triplet excited state HA calculated from Weller's equation is also less than zero (-1.21 eV), indicating that this process should also be feasible. In the system of Fig. 7 we observed that the rise in the absorption revealing the formation of the semiquinone radical anion accompanied the decay of the excited triplet state HA. This implied that creation of the semiquinone radical anion could also be processed through quenching of the excited triplet of HA by DEA in the system of Fig. 7 and the



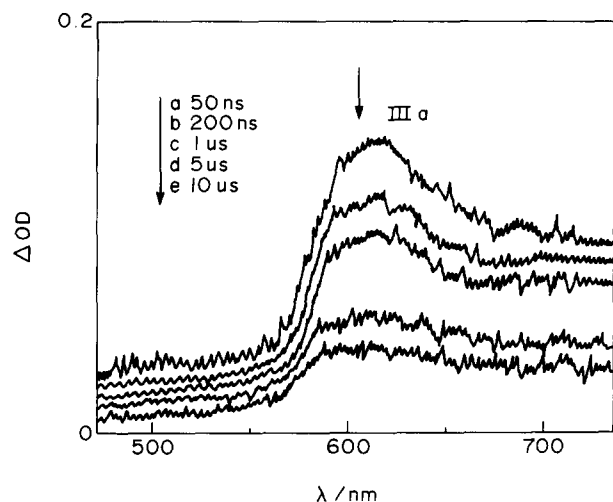


Fig. 8. Time-resolved transient differential absorption spectra of the interaction between HA and DEA in CH_3CN at room temperature ($[\text{HA}] = 3.5 \times 10^{-4} \text{ mol l}^{-1}$, $[\text{DEA}] = 3.4 \times 10^{-2} \text{ mol l}^{-1}$, Ar saturated for 30 min, $\lambda_{\text{ex}} = 355 \text{ nm}$). The delay times after the pulses are shown above the spectra.

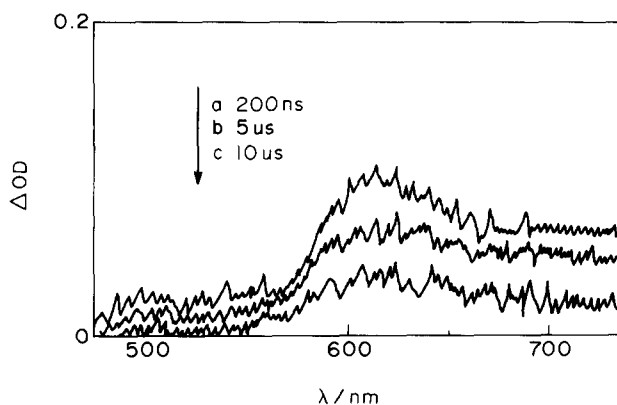


Fig. 9. Time-resolved transient differential absorption spectra of the interaction between HA and DEA in CH_3CN at room temperature ($[\text{HA}] = 0.8 \times 10^{-4} \text{ mol l}^{-1}$, $[\text{DEA}] = 3.4 \times 10^{-2} \text{ mol l}^{-1}$, Ar saturated for 30 min, $\lambda_{\text{ex}} = 355 \text{ nm}$). The delay times after the pulses are shown above the spectra.

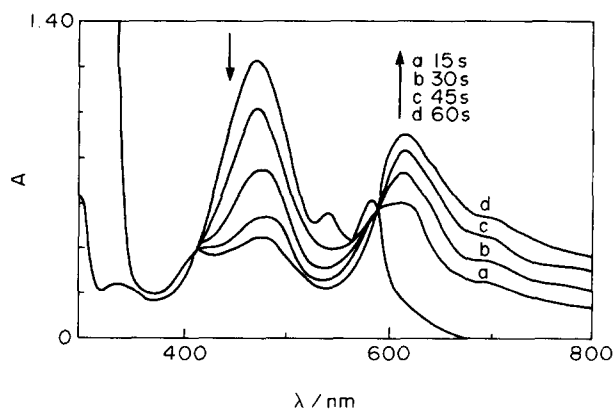


Fig. 10. The absorption spectral changes observed on photoreduction of HA ($5 \times 10^{-5} \text{ mol l}^{-1}$) by EA ($5 \times 10^{-3} \text{ mol l}^{-1}$) in deaerated DMF; irradiation times of 0 s, 15 s, 30 s, 45 s, 60 s were as shown above the spectra.

value of the electron transfer rate constant k_{et}^{T} from the triplet is about $3.99 \times 10^7 \text{ M}^{-1} \text{ s}^{-1}$.

Spectral changes that resulted from different concentrations of DEA and HA used in CH_3CN were also studied and are shown in Fig. 8 and Fig. 9. No $\text{T}_1\text{-T}_n$ absorption and only absorption of the semiquinone radical anion of HA were detected, indicating more complete quenching of excited singlet state HA by more concentrated DEA. Because of the more dilute solution of HA ($8 \times 10^{-5} \text{ mol l}^{-1}$) used in the system of Fig. 8, the intensity of absorption of the semiquinone radical anion of HA observed was much lower.

No exciplex fluorescence even in non-polar solvents can be determined for the HA-DEA system. On the basis of the discussion above, a plausible photolysis mechanism of the interreaction between HA and DEA was proposed (see foot of preceding page).

Moreover, it is currently accepted that the primary processes in the mechanism of the photoreduction of quinones by amines involve two steps. The first step is an electron transfer generating the radical anion of the quinones and the radical cation of the amines. This in turn is followed by proton transfer resulting in the formation of the semiquinone and amine radicals. In our experimental condition, the ESR signals recorded in photolysis of HA or HB and DEA in polar solvents are assigned to the semiquinone radical anions and not to the semiquinone radicals, indicating that proton transfer is not observed. This may be explained by strong intramolecular hydrogen bonding between quinonoid carbonyl and hydroxyl groups in HA and HB, reducing the acceptance of the proton by $\text{HA}^{\cdot-}$ and $\text{HB}^{\cdot-}$. An and coworkers proved that the semiquinone radical (HA) formed from protonation of $\text{HA}^{\cdot-}$ (at $\text{pH} < 7$) with shorter lifetime could not be detected by ESR in our experimental conditions [25]. In addition, the interactions of HA and EA or AN were examined by UV-visible (Fig. 10), ESR and fluorescence spectroscopy (Table 1) in solvents of various polarities and the electron transfer process was also observed in the same experimental conditions.

4. Conclusion

On the basis of a study of fluorescence quenching and calculation of free energy changes, it has been predicted that the excited state HA or HB can accept an electron from ground state DEA. Observation of ESR signals of semiquinone radical anions with resolved hyperfine structure on illumination ($\lambda = 550 \text{ nm}$) of HA or HB and DEA in anaerobic DMSO and CH_3CN solutions provided experimental evidence for this deduction. The absorption band of HA observed by UV-visible spectroscopy is at around 620 nm. When the air was caused to re-enter the photoreduction system, the HA was reversed back quantitatively to HA. Moreover, the examination of nanosecond transient absorption spectra of HA and DEA in CH_3CN and DEA provided further support of this deduction. The transient absorption spectrum of the semiquinone radical anion of $\text{HA}^{\cdot-}$ ($\lambda_{\text{max}} = 620 \text{ nm}$)

was observed on photolysis of different concentrations of HA and DEA used, and the rise in the absorption spectrum revealed that formation of the semiquinone radical anion accompanied the decay of the excited triplet of HA. This implied that the semiquinone radical anion could be created by electron transfer between ground state DEA and both excited singlet and triplet HA. In the less polar solvent CHCl_3 , no semiquinone radical could be detected by ESR or transient absorption spectroscopy.

Acknowledgement

This project was supported by the National Natural Science Foundation of China.

References

- [1] X.Y. Wan and Y.T. Chen, *Kexue Tongbao*, 24 (1980) 1148–1149.
- [2] W.S. Chen, Y.T. Chen, X.Y. Wan, E. Frienderichs, H. Puff and E. Breitmaier, *Liebigs Ann. Chem.*, (1981) 1880–1885.
- [3] M.H. Zhang, S. Chen, J.Y. An and L.J. Jiang, *Chin. Sci. Bull.*, 34 (1989) 401–406.
- [4] Z.J. Diwu and J.W. Lown, *Photochem. Photobiol.*, 52 (1990) 609–616, and references cited therein.
- [5] N.W. Fu, Y.X. Chu, L.Y. Yian, J.Y. An and Z.J. Diwu, *Chin. J. Oncol.*, 10 (1) (1988) 80.
- [6] N.W. Fu, Y.X. Chu and J.Y. An, *Acta Pharm. Sci.*, 10 (4) (1989) 371–373.
- [7] Z.J. Wang, L. Ma, M.H. Zhang and L.J. Jiang, *Chin. Sci. Bull.*, 37 (8) (1992) 1007–1011.
- [8] Z.J. Diwu and J.W. Lown, *J. Photochem. Photobiol. A, Chem.*, 69 (1992) 191–199.
- [9] Z.J. Diwu and J.W. Lown, *J. Photochem. Photobiol. A, Chem.*, 64 (1992) 273–287.
- [10] Z.J. Diwu, *J. Photochem. Photobiol. A, Chem.*, 61 (1995) 529–539.
- [11] J.N. Ma, L.J. Jiang and M.H. Zhang, *Chin. Sci. Bull.*, 34 (1989) 1176–1181.
- [12] K.H. Zhao and L.J. Jiang, *Youji Huaxue*, 9 (1989) 252–254.
- [13] *CRC Handbook Series in Organic Electrochemistry*, Vol. I, CRC Press, Boca Raton, FL, Louis Meites, Petr-Zuman.
- [14] J.B. Birks, *Photophysics of Aromatic Molecules*, Wiley-Interscience, New York, 1970.
- [15] J.M. Chen, T.I. Ho and C.Y. Mou, *J. Phys. Chem.*, 94 (1990) 2889.
- [16] B. Legros, P. Vandereecken and J.Ph. Soumillin, *J. Phys. Chem.*, 95 (1991) 4752.
- [17] M.A. Fox and M. Chanon (eds.), *Photoinduced Electron Transfer*, Elsevier, Amsterdam, 1988.
- [18] J.R. Bolton, N. Mataga and G.L. McLendon (eds.), *Electron Transfer in Inorganic, Organic and Biological Systems*, American Chemical Society, Washington, DC, 1991.
- [19] R.A. Marcus, *J. Chem. Phys.*, 24 (1956) 966.
- [20] R.A. Marcus, *Annu. Rev. Phys. Chem.*, 15 (1964) 155.
- [21] J.Y. An, K.H. Zhao and L.J. Jiang, *Sci. China (Ser. B)*, 34 (1991) 1281–1289.
- [22] Y.Z. Hu, J.Y. An, L. Qin and L.J. Jiang, *J. Photochem. Photobiol. A, Chem.*, 78 (1994) 247–251.
- [23] N. Orbach, R. Polasshnik and M. Ottolenghi, *J. Phys. Chem.*, 765 ((1972) 1133–1139.
- [24] J.N. Ma, L.J. Jiang, M.H. Zhang and Q. Yu, *Chin. Sci. Bull.*, 34 (1989) 1442–1448.
- [25] Y.Z. Hu, J.Y. An and L.J. Jiang, *Sci. China (Ser. B)*, 37 (1994) 15–28.